LAND-BASED MARGINAL ICE CLIFFS: FOCUS ON KILIMANJARO

Michael Winkler, Georg Kaser, Nicolas J. Cullen, Thomas Mölg,
Douglas R. Hardy and W. Tad Pfeffer

With 9 figures
Received 27. Febuary 2010 · Accepted 23. May 2010

Summary: Land-based ice cliffs are intriguing features at the margins of glaciers around the world, but little is known about mechanisms of their formation and maintenance. A review on those ice cliffs, which are mostly associated with dry calving events, is presented. The focus is on the persistent, rarely-calving ice cliffs on the plateau glaciers of Kibo, the main peak of the Kilimanjaro massif (3°S, 37°E), Tanzania. Areal glacier shrinkage on Africa's highest peak is closely linked to the recession of these ice cliffs and in order to extract climate change details from the plateau glaciers on Kilimanjaro, the sensitivity of the cliffs to climate fluctuations must be understood. Modelling solar irradiance, in conjunction with on-site measurements, revealed that direct insolation is the reason for (1) the predominant zonal alignment of the ice cliffs and (2) their bimodal annual recession. The former peculiarity occurs because near the equator steep north- and south-facing slopes receive only little solar energy, which prevents strong ablation. The bimodal recession pattern is caused by the particular annual path of the sun in the tropics, which either induces strong direct insolation on the Kilimanjaro ice cliffs from sunrise to sunset ("sunlit period"), or comparatively low (or no) direct insolation all day ("shaded period"). A 26 m high, 69° steep, and approximately south-facing sample cliff has been surveyed by terrestrial photogrammetry. The daily direct maximum insolation threshold between sunlit and shaded periods at the sample cliff is about 680 Wm^{-2}. During the shaded period from March 4th to October 11th, where mean recession is only 1.4 cm/month, daily maximum insolation at the inclined sample cliff surface is below this threshold. During the sunlit period (mean recession rate ~13 cm/month) daily insolation maxima exceed this threshold.

Zusammenfassung: Eiskliffe an Gletscherrändern sind faszinierende Erscheinungen, die weltweit existieren, auch am Festland. Trotzdem ist wenig über ihre Entstehung und den Grund für ihre Formbeständigkeit bekannt. Ein Überblick über die „landbasierten" Eiskliffe, die meist mit „trockenem Kalben" in Verbindung stehen, wird präsentiert. Der Schwerpunkt liegt dabei auf der Beschreibung der beständigen und selten kalbenden Eiskliffe der Plateaugletscher am Kibo, dem Hauptgipfel des Kilimandscharo-Massivs (3°S, 37°E) in Tansania. Der Rückgang der Gletscherfläche ist dort eng mit dem lateralen Rückzug dieser Eiskliffe verbunden, und um von den Veränderungen der Plateaugletscher am Kilimandscharo auf Klimaänderungen schließen zu können, muss die Sensitivität der Kliffe auf Klimaschwankungen verstanden werden. Die Modellierung der solaren Bestrahlungsstärke und Messungen vor Ort zeigen, dass die direkte Sonnenstrahlung sowohl der Grund für die vorwiegend zonale Ausrichtung der Eiskliffe als auch für das bimodale Rückzugsmuster im Laufe des Jahres ist. Ersteres ergibt sich, weil auf steile Nord- und Südhänge nahe dem Äquator nur wenig solare Strahlung einfällt, weswegen dort die Ablation verringert ist und derart exponierte Steilhänge oder Kliffe auf Dauer erhalten bleiben. Das bimodale Rückzugsmuster wird durch den speziellen Lauf der Sonne in den Tropen verursacht: entweder es trifft den ganzen Tag über starke direkte Strahlung auf die Eiskliffe am Kilimandscharo („besonnte Periode") oder verhältnismäßig wenig bis gar keine („Schattenperiode"). Ein 26 m hohes, 69° geneigtes und ungefähr nach Süden exponiertes Eiskliff wurde photogrammetrisch vermessen. Der Grenzwert für den täglichen Maximalwert der direkten kurzwelligen Bestrahlungsstärke an diesem Kliff zwischen den beiden Perioden ist 680 Wm^{-2}. Während der Schattenperiode vom 4. März bis zum 11. Oktober liegt die mittlere Rückzugsrate bei 1,4 cm/Monat und der genannte Grenzwert wird nicht überschritten. Während der besonnten Periode beträgt die mittlere Rückzugsrate rund 13 cm/Monat und die Tagesmaxima der solaren Bestrahlungsstärke übersteigen 680 Wm^{-2}.

Keywords: Ice cliffs, Kilimanjaro, glacier retreat, dry calving, solar radiation model, terrestrial photogrammetry, tropical glaciers

1 Introduction and background

1.1 Land-based ice cliffs: general considerations

Dry, land-based ice cliffs are found at the margins of ice masses all around the globe. They exist on steep slopes (e.g. at hanging glacier fronts) as well as over flat ground and ablation by "dry calving" is characteristic for most of them. Melting and sublimation are two other important ablation processes at the cliffs located on rather flat ground, but play a subordinate role at cliffed margins over

steep terrain where the interaction between ice flow and calving governs cliff occurrence and shape (Pettit et al. 2006). In the following, only ice cliffs over flat and slightly inclined ground will be addressed.

In the Arctic such cliffs have been described in Northwest Greenland e.g. by White (1958), Hooke (1970) and Goldthwait (1956, 1971), and on Ellesmere Island, Canada, by Greely (1886) and Souchez (1971). (Pictures of land-based cliffs on Axel Heiberg Island, Canada, can be found on www.swisseduc.ch/glaciers.) In Antarctica, e.g., Bull and Carnein (1969), Chinn (1987), Lewis et al. (1999) and Pettit et al. (2006) have studied land-based ice cliffs in the McMurdo Dry Valleys, while Diolaiuti et al. (2004) investigated dry calving cliffs at Terra Nova Bay and Fitzsimons and Colhoun (1995) have described them in the Vestfold and Burger Hills. Lliboutry (1956) shows pictures of terminus cliffs in Chile (near Cerro Negro del Olivares), and there are ice cliffs over rather flat ground in the high and arid regions of the Hindukush-Karakorum-Himalaya chain (P. Wagnon and G. Kaser, pers. comm.) as well as at tropical glacier locations, e.g. on Quelccaya Ice Cap, Peru (D. R. Hardy, pers. comm., see cover on Science, Vol 203, Issue 4386, 1979). Notably, one of the earliest descriptions of dry-based ice cliffs appears to come from Kilimanjaro, Tanzania (Meyer 1891). All these ice cliffs show approximately the same height range (ca. 3–50 m) and all exist in dry and cold environments.

The physical reason for stationary ice cliffs is a distinct interaction between ice flow, accumulation at the faces and the ablation processes of calving, melting and sublimation (Pettit et al. 2006). Therefore, cliff recession (R, defined as positive towards the cliff face) can be written as the negative sum of surface mass balance (SMB) and ice flow (IF), with SMB and IF defined as positive away from the cliff face:

$$R = -(SMB + IF) \qquad \text{Equation 1}$$

The mass balance of the cliff surface is the difference between accumulation and ablation. Accumulation occurs through deposition of water vapor (d), refreezing meltwater flowing off the flatter parts of the ice body or trickling from higher sections of the cliff (r) and solid precipitation accumulating on small scale terraces or ledges at the cliff faces (a). Ablation is the combination of melt (m), sublimation (s), calving (c) due to ice flow, and ice grains falling off the cliff (f) due to melting at the grain boundaries, forming cones at the cliff base:

$$SMB = d + r + a - m - s - c - f \qquad \text{Equation 2}$$

Energy balance studies of terminus cliffs in the McMurdo Dry Valleys, Antarctica, by Chinn (1987, on Wright Lower Glacier) and Lewis et al. (1999, on Canada Glacier) revealed a 2 to 6 times (in some cases even 8 times) higher ablation at the cliff faces than at adjacent slightly inclined glacier surfaces during summer. They attribute this difference to lower wind speeds and higher specific humidity at the bottom of the cliffs and lower parts of their faces (not at the upper edges), resulting in decreased sublimation rates and enhanced melting, which is approximately eight times more effective than sublimation in terms of mass loss (latent heat of sublimation is 8.5 times higher than that of melting). In addition, incoming longwave radiation and net-shortwave radiation are higher at the cliff faces due to absorbed radiation emitted from bare ground and lower albedo, respectively. During the austral winter no melting but moderate sublimation occurs on the Antarctic glacier surfaces, including the ice cliffs.

In the following, the marginal ice cliffs on Kilimanjaro are described as a particular case of non- or rarely-calving land-based ice cliffs. Historical publications dealing with the cliffs are reviewed and a background of present knowledge on cliff face mass and energy balances, as well as cliff orientation is provided. The motivation for investigating the Kilimanjaro ice cliffs is given in section 1.3. In section 2 we describe the study site and our methods to further characterize the cliffs and to evaluate the findings of former publications. We focus on the microclimate at the cliffs, the role of insolation[1)], a digital cliff surface model derived from terrestrial photogrammetry, and point measurements of ice cliff recession. The results are presented in section 3, and conclusions and outlook are given in section 4.

1.2 Kilimanjaro ice cliffs: an overview

The Kilimanjaro massif (3°04'S, 37°21'E) consists of three volcanic peaks: Shira, Mawenzi and Kibo, the latter representing Africa's highest moun-

[1)] Insolation, interchangeably used with "solar irradiance" and "incoming shortwave radiation", is defined as radiant power emitted from the sun being incident on a surface of a certain area [W/m²].

tain (5895 m a.s.l.). At present, glaciers only exist on Kibo, with an areal extent of 1.85 km² in 2007 (Thompson et al. 2009) which has been decreasing at least since the late 19th century (Osmaston 1989). Throughout the history there has been more ice cover on the Western parts of the Kibo summit cone than on the Eastern parts, which is due to the diurnal cycle of local circulation and cloudiness (e.g. Hastenrath and Greischar 1997). Two glacier systems can be clearly distinguished (Geilinger 1936; Kaser et al. 2004; Cullen et al. 2006): (1) slope glaciers that flow (slowly) down the flanks of the evenly shaped volcano, and (2) plateau glaciers situated on the rather flat crater plateau above 5700 m a.s.l. (Fig. 1). The Northern Ice Field (NIF, Figs. 2–4) is situated partly on the plateau and partly on the slopes and it is considered unlikely that there is a dynamic connection between the slope and plateau portions of the NIF (Kaser et al. 2004). In the late 1980's an ice-free gap in the NIF appeared (Hastenrath and Greischar, 1997) which opened to the west around 2004 creating a large canyon feature for yet unknown reasons (Cullen et al. 2006). Today the NIF is almost split up into two independent entities, a southern and a northern, slightly smaller one, both still having a plateau and a slope portion (Fig. 2 in Thompson et al.

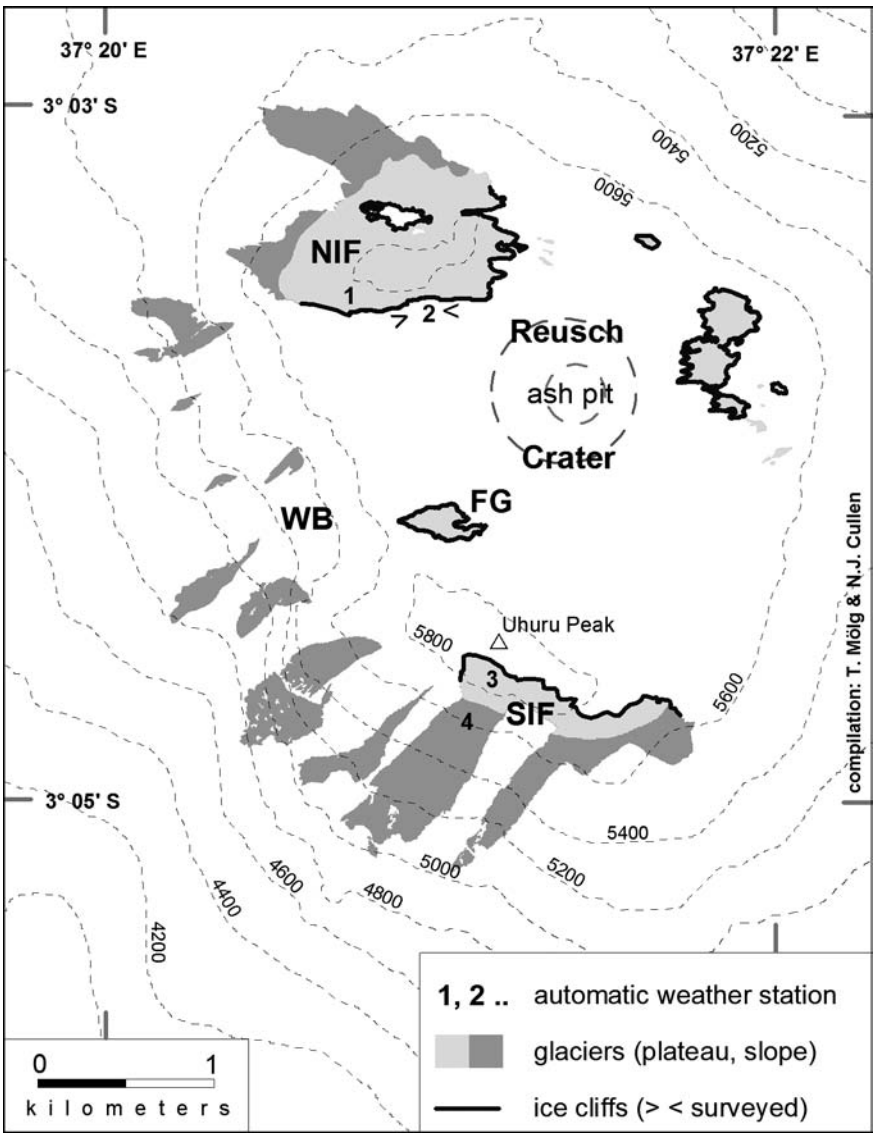

Fig. 1: Map with Kibo glacier extent from 2003. Note the different shading of plateau and slope glaciers. Plateau ice cliffs are marked with bold lines and the surveyed sample cliff is indicated by the two arrows. The numbers 1–4 refer to the automatic weather stations. NIF=Northern Ice Field, SIF=Southern Ice Field, FG=Furtwängler Glacier, WB=Western Breach

Fig. 2: Overview picture of the camp at the southern margin of the Northern Ice Field (NIF) with the sample cliff framed in dashed lines and the cliff station encircled. The photograph was taken by M. WINKLER on January 29th, 2009 at 5 pm local time, looking to the Northeast from a distance of about 300 m to the cliff station

2009). Complete separation of the NIF is likely to happen within the next few years. To assess glacier change on Kilimanjaro, slope and plateau glaciers must be distinguished from each other (CULLEN et al. 2006).

Vertical and near-vertical cliffs occur at the ice margins of the plateau glaciers and at the upper ends of the high-reaching slope glaciers. Some of them also exist below the summit region at the slope glaciers, especially at the ice masses in the Western Breach (WB), but in general they get less frequent with decreasing altitude. Interestingly, the two separating parts of the NIF have been terminated by cliffs since the very beginning of the split process and presumably, they are the highest ice cliffs (>40 m) found on Kibo (cf. Fig. 4).

Significant accumulation on the cliff faces is not possible: water vapor deposition (*d*) is considered to be negligible (KASER et al. 2004) and solid precipitation (*a*) only plays a minor role because the area where snow and graupel can accumulate is very small compared to the whole cliff surface area. Refreezing of meltwater (*r*) originating from the flat plateau and the development of frozen waterfalls at the cliff is difficult to quantify but appears to be a local phenomenon mostly restricted to the upper parts of the cliffs. Another peculiarity at the margins of the plateau glaciers on Kibo is that calving (*c*) is unusual. Nearly all of the brief episodes of ice block disintegration are related to collapses of fragile ice structures rather than calving events, that are caused by ice flow. Recently observed ice break-offs, like on January 24, 2003 at Furtwängler Glacier photographed by V. Keipper (D. R. HARDY, pers. comm.), are clearly connected to sudden outbursts of ponding water that destabilize a marginal cliff. The water accumulation was either due to localized and temporary volcanic activity or due to melting without sufficient refreezing or runoff which – in this case – cannot be connected to any recent climatic changes.

Ice flow (*IF*) is of minor significance on Kilimanjaro because of the thin ice and the low slopes on the summit plateau (KASER et al. 2004). Textures in the basal ice exposed at the margins show no evidence of deformation. There is no sign of either basal debris erosion or entrainment nor are any moraine-like deposits evident. The rarity of calving events further points to the insignificance of *IF* on the plateau glaciers. In polar regions the interaction of calving processes and ice flow at least partly necessitate the occurrence of terminal ice cliffs. The non- or rarely-calving ice cliffs on Kilimanjaro seem to be a peculiarity and there must be another reason for their existence. KASER et al. (2004) attribute the onset of their formation to fumarole activity in the Reusch Crater (Fig. 1), which was described by SPINK (1944) in detail, but also to differential ablation driven by incoming shortwave radiation (e.g. KRAUS 1972). PETTIT et al. (2006) developed a conceptual model for glacier terminus morphologies based on observations from Taylor Glacier, McMurdo Dry Valley, Antarctica. Their model also allows the existence of non-calving ice cliffs, where ablation is governed by melting and sublimation.

For the reasons mentioned above, we neglect accumulation, calving and ice flow, and ice cliff recession on Kilimanjaro can thus be expressed as

$$R_{Kibo} = m + s + f \qquad \text{Equation 3}$$

Equation 3 suggests that once ice cliffs on Kibo are formed they retreat due to melting, sublimation and grain fall-out. This is in accordance with observations which show that R_{Kibo} is always positive (sec-

tion 3). Continuous shrinkage of horizontally projected glacier area on the summit plateau is unavoidable as a consequence of this persistent lateral retreat.

Despite the continuous recession, Kilimanjaro's ice cliffs have existed and kept their shape for at least 130 years. They have been described, painted and photographed by early explorers (e.g. Meyer 1891; Klute 1920; Jäger 1931; Geilinger 1936; Spink 1944) and also reported in more recent publications (e.g. Hastenrath 1984; Kaser et al. 2004). In general, authors agree that cliff heights range between about 3 and 50 m. Some report thinning of the Kibo glaciers but mostly it is not clearly attributed to thinning of the plateau glaciers, which would be equivalent to a decrease in cliff heights. Others, e.g. Thompson et al. (2009) and Hastenrath (2010), calculate a mean topography decrease at the NIF. Hastenrath (2010) reported a 14.51m thinning between 1962 and 2000 (38cm/year) for a rectangular section on the NIF. However, as the studied area includes the present NIF gap (H. Brecher, pers. comm.) these mean thinning values do not represent surface ablation. They include the opening of the gap and associated lateral retreat of the cliffs enclosing the gap. Only Geilinger (1936) undoubtedly (but qualitatively only) mentions thinning of the summit plateau ice bodies from 1901 to 1929 and, at an accelerated rate, from 1929 to 1935. Still, analyses of publications between 1880 and today (see Kaser et al. (2004) for references) reveal no significant change in the range of cliff heights during this period.

Strikingly, the cliffs are mainly either north- or south-facing (see Fig. 4; frontispiece in Hastenrath 1984; Kaser et al. 2004) and while some marginal cliffs extend over the full ice thickness, others, set back from the margin, rise from the flat plateau glaciers creating their typical terraced shape (Fig. 4; Jäger 1931; Humphries 1959; photographs from 1974 in Hastenrath 1984; Kaser et al. 2010). In addition to the lack of calving, the preference for either south- or north-facing cliffs is a peculiar feature on Kibo. Hooke (1970) mentions a tendency of the ice cliffs in Northwest Greenland to be systematically oriented parallel to the main wind direction, but wind can be ruled out as the reason for the distinct orientation of the ice cliffs on Kilimanjaro because wind speeds are generally low (Mölg et al. 2009a).

Depending on season, the zonally oriented vertical cliffs on near-equatorial Kilimanjaro are either irradiated by direct sunlight during all daytime or not at all (section 3). Jäger (1931) described the consequences for ablation at the ice cliffs by connecting two early observations: Uhlig (1908) reached the Johannes Notch at the crater rim of Kibo on August 2nd, 1904 and noted that "[t]he south-facing, vertical ice cliff at the Johannes Notch […] is showing hardly any signs of melting or icicles (shady side in August)" and Miss Wendtlandt (Jäger 1931, 295) described "[s]tronger, vertical melt channels and icicles on the ice cliff, which is facing the sun now" during her climb on December 1st, 1927. Kaser et al. (2004) elaborate this periodic change between melt and non-melt conditions at Kibo's ice cliffs: during the boreal (austral) summer north-facing (south-facing) cliffs are irradiated by direct sunlight during daytime, which provides enough energy to initiate melting at the cliff faces although the air temperature is below freezing. Meltwater drops develop and run down the faces. The water either refreezes when it is exposed to cold air (icicles can form), evaporates after ponding at the cliff base, or infiltrates into the ash. This situation is comparable to the situation in the McMurdo Dry Valley in summertime, as discussed above. In contrast, during the boreal (austral) winter north-facing (south-facing) cliffs are irradiated by direct sunlight only at very low angles. Insufficient energy is available to bring the cliff face up to melting. Only sublimation occurs and ablation is reduced significantly. This situation is comparable to conditions in the McMurdo Dry Valleys in wintertime.

1.3 The motivation for investigating Kilimanjaro ice cliffs

The assumptions leading to Eq. 3 reveal that ice cliffs on Kilimanjaro are forced to retreat as soon as they exist due to ablation processes (*m, s, f*) and the lack of accumulation and ice flow. This has drastic consequences for the plateau glaciers' areal extent. According to Kaser et al. (2010), only a large increase in precipitation can explain a continuous buildup of new ice entities and prevent glacier wastage on Africa's highest mountain. Because the last 130 years experienced relatively dry climate conditions (e.g. Mölg et al. 2009a) no ice buildup was possible and the area of existing ice entities shrank due to inevitable cliff recession and related separation of ice bodies into small and quickly disintegrating entities. In order to extract a climate change signal from changes in total glacier extent on Kilimanjaro it is key to understand the micrometeorological conditions under which the cliffs develop, persist and may decay, and how these conditions are connected to East African tropospheric climate (Mölg et al. 2003; Kaser et al. 2004; Cullen et al. 2006). Evaluation

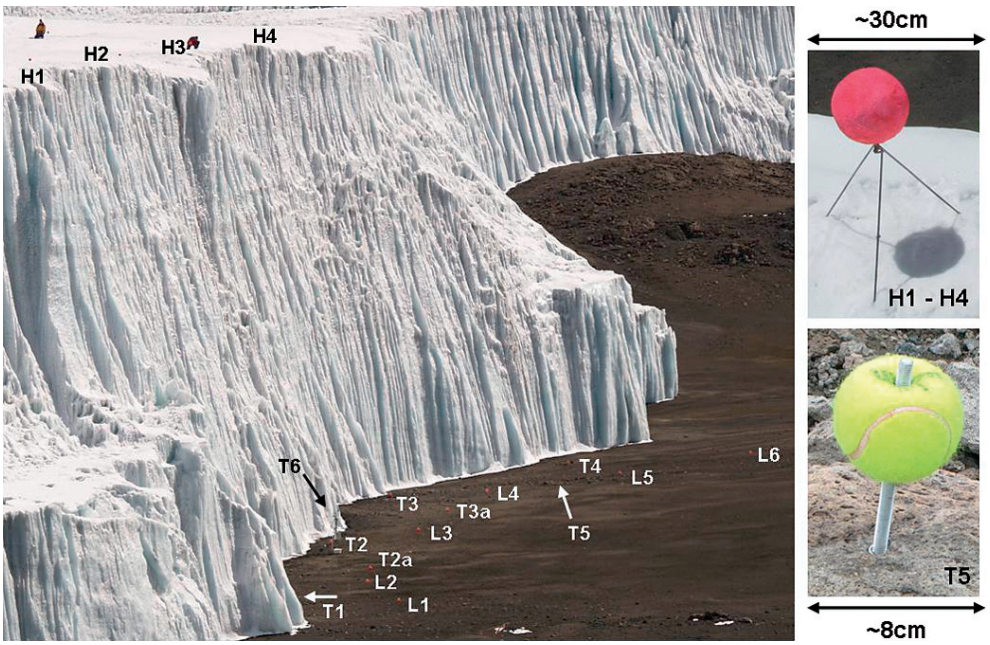

Fig. 3: Overview of the markers for the photogrammetric survey. The photograph was taken by G. KASER on January 30th, 2009 at 10 am from the western edge of the crater rim looking to the East. Note that the survey used for this study was made with the same setting, but in October 2009. The distance to the cliff station is about 500 m, with seated people on top of the cliff providing useful references for the scale of the image. T6 is mounted on the cliff station, which is hardly visible on the picture. Note the strong distortion due to the zoom lens, which makes the surface appear rougher than it is

of all drivers of the recession is necessary since little is known about the energy balance of the cliffs, and glaciers with cliffed margins are known to respond differently to climatic changes than glaciers with moderately sloped termini (PETTIT et al. 2006). This paper provides a qualitative and quantitative description of the Kibo ice cliffs, their recession, and the microclimate near them.

2 Study site and methods

In February 2000 an automatic weather station (AWS) was installed on the flat top of the Northern Ice Field (NIF) at 5794 m a.s.l. by Douglas R. HARDY, University of Massachusetts (MÖLG and HARDY 2004). This station (AWS1 in Fig. 1 and Fig. 4) provides a unique and continuous data set until the present day. In February 2005 two additional AWSs were set up by the Tropical Glaciology Group, University of Innsbruck (see Fig. 1): AWS2 was placed approximately 2–4 m out from the base of a south-facing cliff at the NIF (~5750 m a.s.l.) and AWS3 was situated on the upper slopes of the Southern Ice Field (SIF) at 5873 m a.s.l. In January 2009 another station (AWS4) was installed on the mid slopes of Kersten glacier (SIF) at an elevation of about 5600 m a.s.l. in order to estimate vertical gradients of precipitation, temperature and humidity along the glacier between AWS3 and AWS4. In this study, data from AWS2 and AWS3 are used. The instruments used at both of them are identical and a detailed description of AWS3, which is strongly impacted by the free atmosphere (MÖLG et al. 2009b), can be found in MÖLG et al. (2008, 2009a).

At AWS2, hereafter called "cliff station", air temperature and relative humidity (Rotronic MP100A) are measured at 160 cm, while wind speed and direction (RM Young 05103) are recorded at 225 cm above the bare ash ground. An ultrasonic ranging sensor (Campbell SR50) at 187 cm height continuously records the distance between the station and the cliff, and a radiometer (Kipp and Zonen CNR1) measuring incoming and outgoing shortwave (0.305–2.8 µm) and longwave (5–50 µm) radiation was mounted at 206 cm facing towards and away from the cliff to assess the radiant fluxes on the cliff face. This way of mounting a radiometer was already practiced by LEWIS et al. (1998) in the McMurdo Dry Valleys, Antarctica. All measurements are sampled every minute and stored as half-hourly means on a Campbell CR23X datalogger.

To evaluate the role of insolation at all ice cliffs on Kilimanjaro a model for direct and diffuse solar

irradiance on any arbitrarily oriented surface ($I_\theta = I_{dir} + I_{diff}$) is developed from Iqbal (1983), Young (1994), Sproul (2007), and Mölg et al. (2009c). Equation 29 in Sproul (2007) was used to calculate the cosine of the actual angle of incidence of direct solar insolation ($\cos\theta$) for any surface at any time during the annual cycle. The effect of clouds and reflections from surrounding surfaces are ignored, and it turned out that the remaining diffuse part (I_{diff}) of the insolation is negligible at the altitude of the Kibo summit plateau, as found from AWS data as well (Mölg et al. 2009c). The absorbed fraction of incoming shortwave radiation was not calculated because cliff face albedo is assumed to be quite constant.

The cliff towering 25 m above the cliff station (Fig. 1 and 2) is part of the southern margin of the NIF, which is a continuous south-facing ice cliff that is approximately 1 km in length. About 20 m to the west and 60 m to the east of the station the cliff is rather uniform in terms of height, slope and surface roughness, it has a rather linear basal contact line, and it consists of one continuous face with no terraces or steps. Our studies focus on this section of the cliff, hereafter referred to as "sample cliff" (Fig. 2 and arrows in Fig. 1).

In order to directly measure ablation, three stakes were drilled horizontally into the sample cliff in January 2009 close to the cliff station at 216 cm, 220 cm and 234 cm above the ground, respectively. In combination with R_{Kibo}, directly derived from the sonic ranging measurements, the stake measurements provide a way to estimate potential ice flow around the station that would be a residual in Eq. 3.

As stake and sonic ranging measurements only provide point information, photogrammetric surveys of the sample cliff were carried out in January and October 2009, and additional ones are planned in the future. The October 2009 survey was chosen for a quantitative description of the sample cliff features (see section 3.3). All the photographs were taken with a calibrated DSLR camera (Nikon D200 with 10.2 million pixels) and a 20 mm lens mounted on a tripod. 16 pink styrofoam balls (14 cm diameter) were used for photogrammetric tie points and ground control (Fig. 3 shows an overview). 12 out of the 16, having a tennis ball (6.4 cm diameter) on their tops, were randomly placed on the flat ash ground several meters in front of the sample cliff (T1, T2, T2a, T3, T3a, T4 and L1-6). The remaining four markers were mounted on wired tetrahedrons and placed on the upper edge of the cliff, 39–40 cm above the ice surface (H1–4). One additional tennis ball was put on a threaded rod and fixed in a borehole on a rock outcrop near the sample cliff (T5) and one other (T6) was mounted on top of the cliff station mast. During the first photogrammetric survey in January 2009 all the markers were surveyed with a Leica TCRA 1101 total station and five (T1-5) were permanently marked in the ash ground with spikes. These five can be recovered for subsequent surveys and are the basis of a stationary reference system; other markers were fixed only during the time of an individual survey and provided photogrammetric tie points between images. Additionally, during the October 2009 survey two markers (T2a, T3a) were mounted at exactly the same altitude as T2 and T3, respectively, using a water level gauge. 16 photographs from October 2009, piecewise covering the whole sample cliff and the 18 markers, were used to build a three dimensional reference frame using photogrammetry software (PhotoModeler Scanner). Automatic stereo matching of the photographs leads to a referenced digital surface model (DSM) of the sample cliff.

3 Results

3.1 Observations and microclimate at the ice cliffs

Observations of glaciers on Kilimanjaro during our recent field trips verify the findings reviewed in section 1.2 (for e.g. shape, distinct top edges, and surface roughness). Cliff heights might have generally decreased, but still show the same range of heights (~3–50 m). On the NIF overview image in figure 4A the alignment of the cliffs is indicated. Figure 4B shows a close-up of the NIF gap area with high north-facing cliffs and narrow, linear remnants of ice on the ash ground. Small parts of the margins on the picture are facing to the East (encircled). These and also the west-facing parts of the plateau glaciers (not shown) are characterized by vertical or near-vertical ice cliffs, but their surface is not smooth. These sections are characterized by lamellae-, pillar- or ship's bow-like structures causing the main portion of the cliff surface area to be either north- or south-facing and inducing multiple reflections of shortwave radiation in the grooves and dihedrals.

The microclimate along the cliffs is considerably different from that at the near-horizontal ice surfaces. Figure 5 shows a comparison of mean daily cycles of meteorological key variables between the sample cliff (cliff station data, solid line) and the uppermost slopes of the SIF (AWS3 data, dashed line) based on measurements from February 2005 to

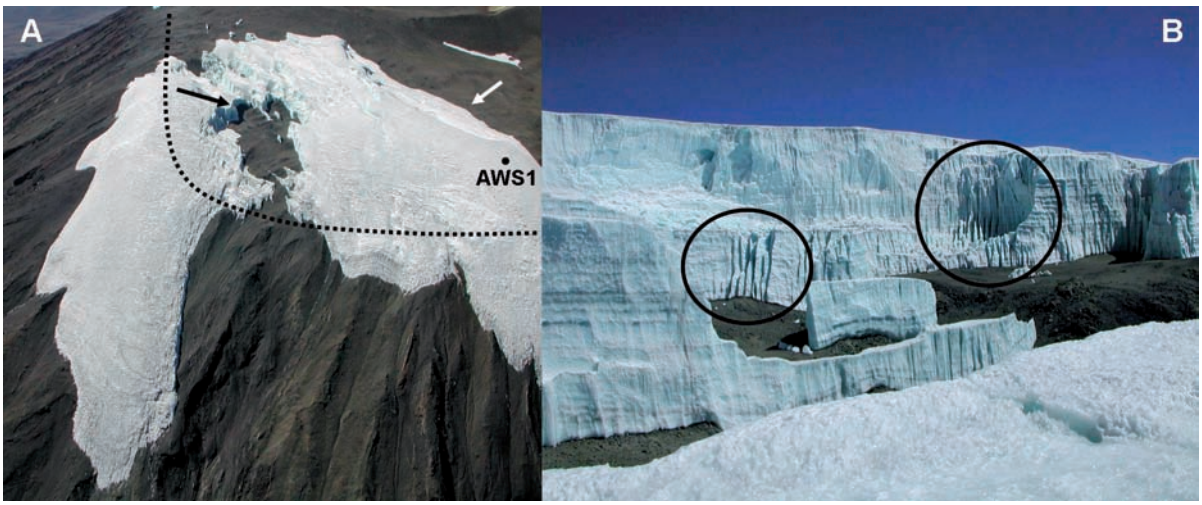

Fig. 4: Picture A shows the Northern Ice Field (NIF) from the air, looking Southeast. The emerging gap in the NIF is clearly visible. The dashed line roughly indicates the crater rim, the border between flat and steep ground and between the plateau and the slope glacier part of the NIF. The white arrow points at the (obstructed) cliff station at the sample cliff and the black arrow shows the location and photographing direction of picture B, which is a close-up of the gap. Note the east-west alignment of the cliff in A and the difference between the smooth north-facing cliffs and the lamellae- and pillar-like structures (encircled) in the east-facing parts of the ice margin in B. (Both photographs were taken by N. J. CULLEN July 2005)

January 2006. Under mean conditions both AWSs experience continuous sub-freezing air temperatures (T_a). Half-hourly AWS3 data show that the free atmosphere is always well below freezing and the cliff station records air temperatures above 0 °C in less than 1% of cases. In the boundary layer between ice cliff and ash ground, wind speeds are very low and radiant fluxes are high during such periods. Nevertheless, ice cliff surface temperatures reach the melting point on most of the days during the sunlit period (KASER et al. 2010). Lower cliff station air temperatures during nighttime are probably due to the formation of a cold reservoir, with a strong inversion in front of the sample cliff after sunset. Low nighttime wind speeds (v) at the cliff and, associated, limited mixing with ambient (warmer) air support this notion.

Water vapour pressure (e) is always low at both AWSs but somewhat lower at the upper slope glacier due to higher wind speeds and stronger mixing with the free atmosphere (details in MÖLG et al. 2009b). Wind speeds are always low at the sample cliff with a small maximum around noon, just before local convection maximizes (MÖLG and HARDY 2004) and wind speeds at AWS3 get decoupled from the prevailing mid-troposheric wind regime, which is characterised by easterlies over Kilimanjaro (MÖLG et al. 2009b).

The bottom graph in figure 5 shows a comparison of incoming longwave radiation (LW_{in}) between the cliff station and AWS3 with respect to the particular ice surface (vertical and horizontal sensor arrangements, respectively). At the upper slopes of the SIF this energy balance component is low because of the cold, dry, and low-density air above Kibo. The ice cliff surface, on the other hand, experiences a large daily cycle with generally high LW_{in} due to radiation emitted from the rather flat ash ground and the surrounding topography, which are strongly heated by absorbed shortwave radiation during daytime when they are snow-free. Thus, longwave radiation emitted to the ice cliff surface is very much reduced during days with snow cover on the crater plateau when ground surface temperatures do not exceed 0 °C.

Low latitudes are characterized by high midday solar elevations all year resulting in small mean optical air masses and, thus, high solar irradiance (I_0) at the surface. The marginal ice cliffs on Kilimanjaro mainly exist at 5600 m a.s.l. or higher, close to the tropical 500 hPa pressure level, where optical air mass is approximately 50% less than at sea level (IQBAL 1983), and direct insolation is significantly increased. Diffuse insolation, on the other hand, is strongly reduced due to low air density, low water vapor pressure and low turbidity (clean air) at Kilimanjaro summit.

The earth's axial tilt is about 23.5°, which means that between 23.5°N and 23.5°S the sun is at the zenith twice a year. On Kilimanjaro (3°S) this happens on March 13th and on October 1st. Midday solar elevation is lowest at the boreal summer solstice (63.5°).

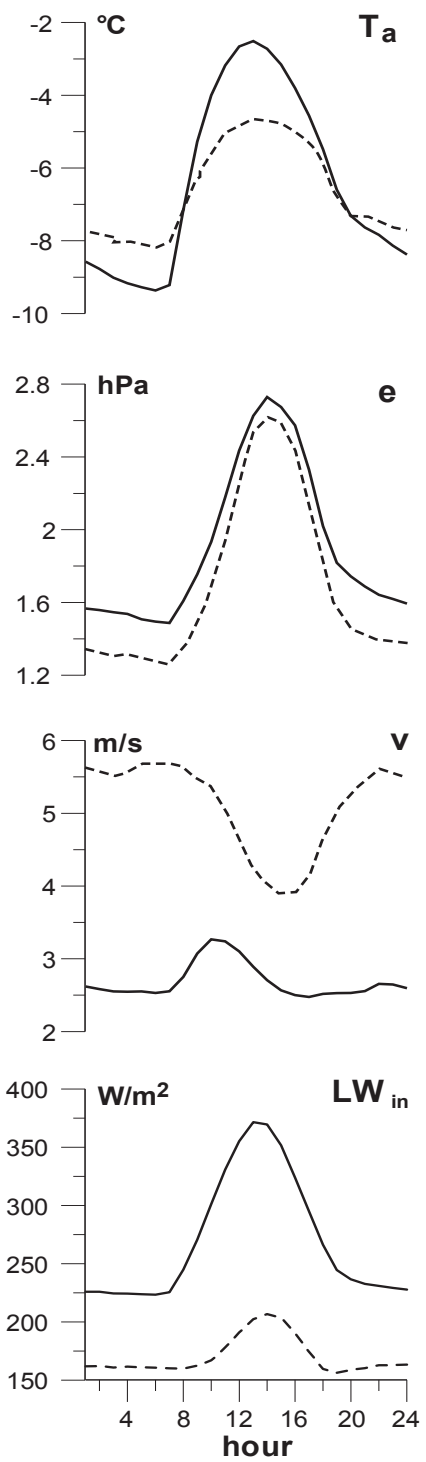

Fig. 5: Mean daily cycles of different meteorological variables at the cliff station (solid lines) and AWS3 at the upper slopes of the Southern Ice Field (dashed lines) based on measurements from February 2005 to January 2006. T_a = air temperature, e = water vapor pressure, v = wind speed, LW_{in} = incoming longwave radiation with respect to the cliff or glacier surface, respectively

The tropics are known for their short sunrises and sunsets due to the large angle between sun path and horizon. On Kilimanjaro the astronomical sun rise is always between 5:55 and 6:05 local apparent time (LAT) in the East (67°–113°) and it sets between 17:55 and 18:05 LAT in the West (247°–293°).

In order to show the different availability of solar energy for differently sloped and exposed ice surfaces on the high and dry top of Kilimanjaro, annual mean insolation for arbitrarily oriented surfaces were calculated, ignoring clouds as a first order approximation (Fig. 6). Horizontal surfaces are much stronger irradiated by the sun than steep ones, and there is a significant difference between vertical west- and east- faces (200 Wm^{-2} annual mean solar irradiance) and vertical north- and south-faces (100 and 70 Wm^{-2}, respectively). Obviously, solar elevation is low during the morning and evening hours resulting in strong insolation on steep east- and west-facing surfaces. Conversely, solar elevations are always high around noon when the sun is near the zenith resulting in low mid-day insolation on all cliff faces. Consequently, steep north- and south-faces are less irradiated by the sun than east- and west-faces. This spatial difference in shortwave energy supply also helps explain long-term changes of plateau glaciation on Kilimanjaro, as simulated by Mölg et al. (2003). A plateau-wide (but cliff-margined) ice cap must disintegrate first in the east and west sectors where east- or west-facing cliff sections dominate (Mölg et al. 2003), which leaves ice remnants primarily in the north and south sectors as we observe today (Fig. 1).

Most of the ice cliffs on Kibo today are either north- or south-facing and they appear to be at least 60° steep. Figure 6 shows that this is indeed the slope-aspect-range that is least irradiated by the sun on an annual average. The slope and aspect of the sample cliff is within this range (section 3.3). Small deviations might be explained by local, asymmetric effects like strong longwave radiation emitted from the slopes of the near-by Reusch Crater (Fig. 1). Flatter slopes and also steep east- and west-facing slopes get more shortwave energy and melt is enhanced. Still, the horizontal surfaces on top of the plateau glaciers are persistent although incoming shortwave radiation is highest at horizontal surfaces. Different from the cliff faces, snow can accumulate on those flat surfaces and, additionally, meltwater is ponding there and refreezes during the nights, which constrains ablation (Mölg and Hardy 2004). Taken together, these processes keep long-term mass changes on horizontal surfaces small compared to that on the ice cliffs.

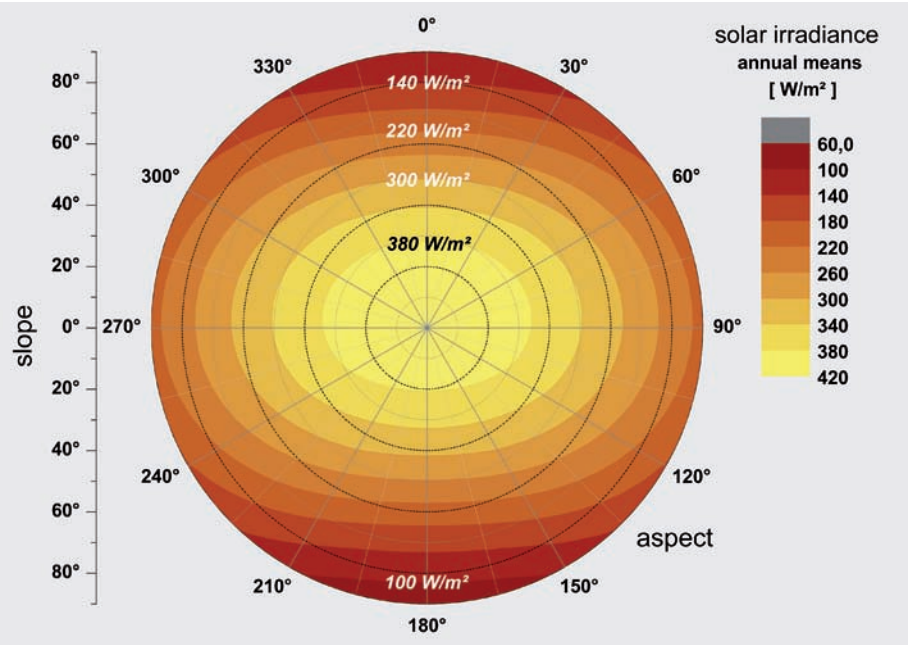

Fig. 6: Annual means of solar irradiance in Wm^{-2} with respect to different slopes and aspects on Kibo. Note the difference between east/west- and north/south-facing slopes. Vertical east- and west-faces receive about 100 Wm^{-2} more solar energy than vertical north-faces and about 130 W/m^2 more than vertical south-faces

3.2 Ice cliff recession

The half-hourly distance measurements between the cliff station and the cliff by the sonic ranging sensor can be interpreted as the net-retreat (R_{Kibo}) of the cliff during a certain period. It clearly shows a bimodal pattern at the sample cliff (Fig. 7). From the beginning of March until mid-October (sun path to the north of Kibo) the retreat rate is only about 1.4 cm/month, during the rest of the year it increases to about 13 cm/month. Thus, the measured distinct recession pattern is directly tied to the solar cycle and reveals that insolation is not only the primary reason for cliff slope and aspect, but also governs their retreat and thus confirms previous exploratory modelling (MÖLG et al. 2003). When the solar declination is greater than about -7°, which is typically the case between March 4th and October 11th, recession rates are low. During the remaining part of the year recession is about 10-times faster. The phase of slow (fast) retreat is associated with a maximum daily solar irradiance (with respect to a plane exposed and sloped like the sample cliff) of less (more) than about 680 Wm^{-2} (Fig. 7). Daily mean solar irradiance is about 210 Wm^{-2} at the transition dates.

The two phases have already been called "shaded" and "sunlit" seasons in previous sections and are characterised by the dominance of two different ablation processes (KASER et al. 2010). During the shaded season only sublimation occurs at the cliff and the cliff surface is dry and cold (<0 °C). There is no meltwater ponding at the cliff base and all the water flowing down from the flat surfaces on top of the plateau glaciers refreezes a few meters after running over the cliff edge. Cones of snow and ice grains at the bottom are small or even absent (except after heavy snowfalls, which are not common (e.g. MÖLG et al. 2009b)). However, even during the shaded season there are only a few days where no direct sunlight hits the sample cliff, but the angle of incidence (θ) is very low (always <25°).

During the sunlit season, in turn, θ is larger and sufficient energy is available to warm the cliff surface to freezing point and initiate melting. Still, sublimation is supposed to consume most of the available energy, but melting is less expensive energetically (about 8.5 times less than sublimation) and, additionally, there is more solar energy available during the sunlit period. These processes favour an accelerated retreat during the sunlit period which is confirmed by point measurements at AWS2 showing an about 10-times faster retreat than during the shaded period (Fig. 7). The ice at the cliff surface starts to melt in the morning leading to a saturated surface, while meltwater draining from the upper, flat plateau trickles down the whole cliff face and ponds at the ash ground at the base (or infiltrates when the ground is not frozen). Cones of ice grains that fall off

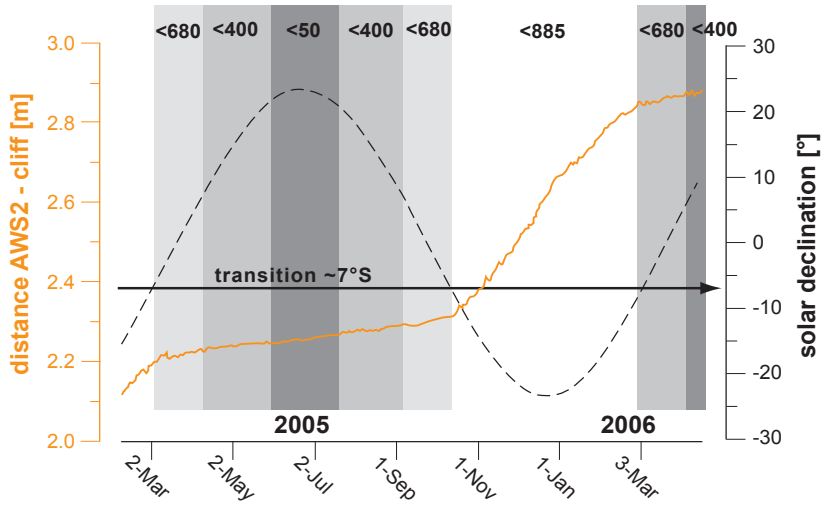

Fig. 7: Comparison of solar declination (black, dashed line) and measured point retreat (orange, solid line). The bars indicate the intervals where maximum daily solar irradiance with respect to a plane with the same slope and aspects as the sample cliff is lower than 50 Wm^{-2} (May 27th–July 18th), lower than 400 Wm^{-2} (April 6th–September 7th), lower than 680 Wm^{-2} (March 4th–October 11th), and between 680 Wm^{-2} and about 885 Wm^{-2} (October 12th–March 3rd). 680 Wm^{-2} denotes the threshold between slow and fast retreat of the cliff (shaded and sunlit season, respectively)

due to melting at the grain boundaries (*f*, defined in section 1.1) develop at the bottom, even if no recent snow has fallen, as described e.g. by JÄGER (1931) and KASER et al. (2004).

On October 8th, 2009 first readings from two of the three stakes, which were drilled horizontally into the ice cliff on January 30th, 2009 were made. The ablation near the cliff station at 216 cm and 234 cm above the ash ground was 22 cm and 19 cm, respectively. Distance measurements provided by the sonic ranging sensor show a mean recession of about 16 cm for the same time period of the years 2005–2008. The rather good agreement between these measurements supports the assumption that ice flow does not play a significant role at least at the sample cliff.

3.3 Photogrammetric survey in October 2009

Model accuracy is considered first. It was estimated by comparing the distances between the markers in the October 2009 photogrammetric model, with the distances measured with a tape in the field. None of the differences were greater than 5 cm and the mean difference was 2 cm (~0.1%). Furthermore, the markers T2 and T3 were installed at exactly the same altitude as T2a and T3a, using a water level gauge. In the photogrammetric model the z-coordinates deviate from the gauge measurements by only 3 mm (at T2/T2a) and 0.3 mm (at T3/T3a). This simple error estimation is sufficient for this study and its results show that the DSM derived from the photogrammetric survey is good enough to make the following analyses.

Sixteen photographs taken in October 2009 were used for a photogrammetric model of the sample cliff. Automatic stereo matching resulted in a cloud of 1.5 million referenced points at the cliff (about 1000 points per m^2). A least square error calculation was used to derive a best-fit-plane for the point cloud. This plane has an aspect of 166° from North and its slope is 69°, which can be interpreted as mean values for aspect and slope of the whole sample cliff. The standard deviation of the point cloud from the plane is 1.26 m, which provides an estimate for the geometrical roughness of the cliff and shows that the sample cliff is rather smooth with no significant jumps in aspect and slope. On the whole, the surveyed cliff area projected onto a vertical plane is roughly 1500 m^2 and cliff height is spatially constant at about 26 m. The main direction of the cliff recession is expected to be horizontal towards 346° (NNW-N).

Using geographical information software the point cloud was converted to a digital surface model (DSM) with 10 cm grid spacing, which is shown in figure 8. The coloring refers to the distance from a zero point (some meters in front of the cliff) along the expected main direction of retreat. Reddish colors indicate close-by sections of the cliff, bluish colors mark the sections that are farther away. The structure of the sample cliff, with its very smooth surface parts and small pillars and gullies, is visible

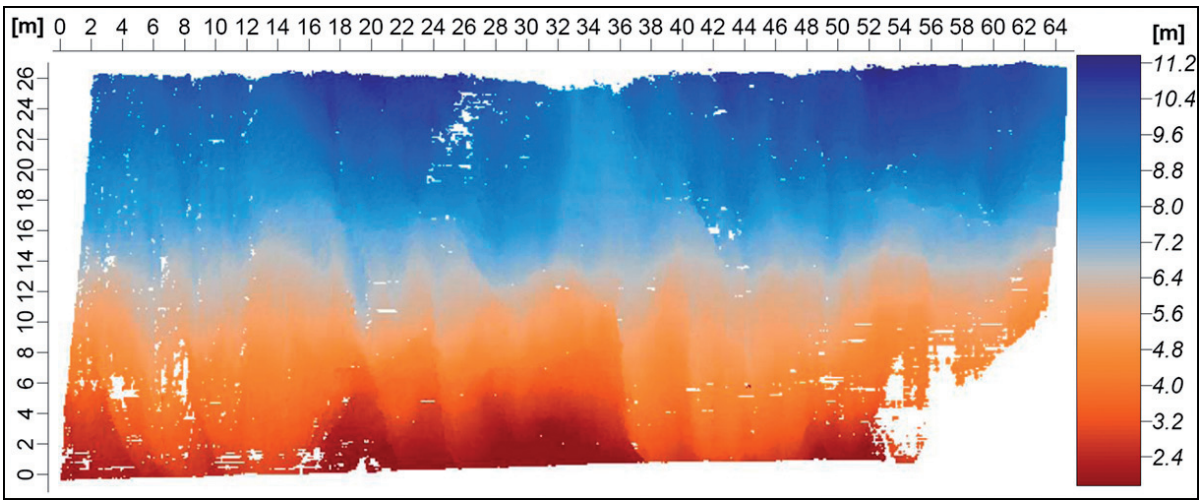

Fig. 8: Digital surface model (DSM) of the sample cliff with 10 cm grid spacing derived from a photogrammetric survey in October 2009. The left axis shows the height of the cliff along a perpendicular axis with an arbitrarily chosen zero point roughly at ash ground level. The upper axis is the distance along the intersection line of the best-fit-plane and the ground level. The colour code shows the offset of the cliff surface along the expected main direction of retreat (see text for details). White pixels represent sections where the automatic matching routine was not successful (e.g. due to low contrast on the photographs). All units are in meters

at the DSM. Steeper parts are indicated by a slow change in color with height.

Using the 10 cm grid a frequency distribution of grid cell aspects and slopes was derived. Figure 9 shows the smoothed result at a scale of 1° × 1° (slope × aspect). The coloring was derived using relative frequencies: 1.0 units correspond to 1/100 per cent of all the 10 cm grid cells having the respective aspect and slope on base of the 1° x 1° raster. 36% of the cliff is between 60°–80° steep, with aspects between 110° and 180° (ESE-S).

4 Conclusions and outlook

Publications on land-based, dry calving marginal ice cliffs have been reviewed and general considerations about their existence and their surface mass balance are presented in this paper. The ice cliffs on the plateau glaciers of Kilimanjaro are introduced as a peculiarity in this context because of the insignificance of ice flow-driven dry calving as an ablation process at their cliff faces.

It is shown that two peculiar observations on the ice cliffs of Kilimanjaro are directly linked to the annual insolation geometry: (1) the pronounced zonal alignment of the ice cliffs and (2) their bimodal annual recession. On vertical or near-vertical, north- or south-facing surfaces annual mean shortwave irradiation is only about half compared to east- and west-facing slopes of the same inclination, and only a quarter compared to flat surfaces. However, snowfall accumulates on horizontal surfaces and a significant amount of meltwater refreezes. These effects conserve the flat glacier parts and the north- and south-facing cliffs, but prevent the long-term occurrence of east- and west-facing cliffs.

The bimodal annual recession is a consequence of the zonal alignment of the cliffs because the sun either irradiates the cliff faces on near-equatorial Kilimanjaro rather strongly (sunlit season), or hardly at all (shaded season). The changes between the two seasons occur when modeled daily maximum solar irradiance at the cliff surfaces gets about as low (or as high) as 680 W/m² in the course of the year. Low retreat rates of about 1.4 cm/month occur during the shaded period and higher rates around 13 cm/month are typical during the sunlit season. Sufficient energy is available to allow 0 °C surface temperatures, which initiates melting around solar noon during the sunlit season, but not during the shaded season, where only sublimation accounts for ablation at the cliffs. As the latent heat of fusion is 8.5-times lower than that of sublimation, much more mass is lost during the sunlit period and recession rates are enhanced. The bimodal retreat results in an annual ice cliff recession in the order of about one meter, consistent with the average 2000–2007 retreat measured along another part of the NIF (Thompson et al. 2009). Due to the lack of significant accumulation at the cliff faces their retreat is irreversible and unstoppable as soon as they are established, and areal shrinkage of the plateau glaciers is an inevitable consequence.

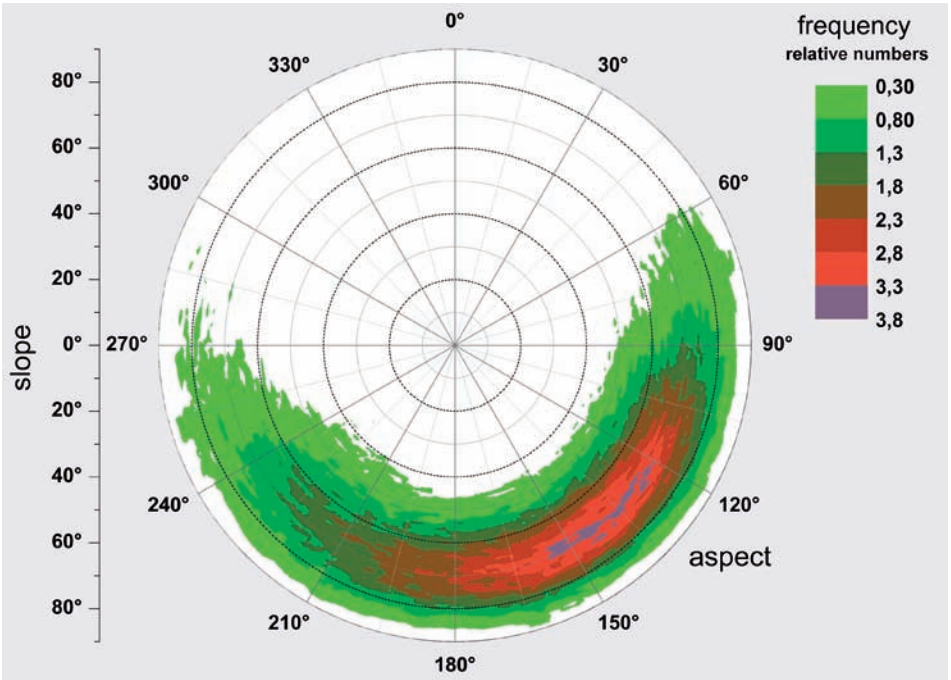

Fig. 9: Frequency of 10 cm grid cells from the digital surface model as a function of slope and aspect. (In the centre of the circle "it is flat", the more one gets to the margin "it gets steeper".) Most parts of the sample cliff are SSE-exposed and about 70° steep

A high resolution photogrammetric survey revealed a mean aspect of 166° from North (SSE-S) and a mean slope of 69° for a 26 m high, 1500 m² cliff section. Upcoming analyses of two more surveys (all made roughly at the transition dates between sunlit and shaded period) will provide an areal recession pattern of the ice cliffs. Small scale differences in retreat will be studied as a function of aspect, slope, height above ground, and insolation phase. This will help develop a cliff surface energy balance model using automatic weather station data from the bottom of the surveyed cliff as input. Ice cliff sensitivity to local climatic variability will be assessed and thresholds for the meteorological key variables (solar irradiance, water vapor pressure, and air temperature), which determine whether ice cliffs persist or decay and, thus, indicate a change in the nature of ice ablation on Kilimanjaro, will be estimated.

Acknowledgements

This study was funded by the Austrian Science Foundation (FWF Grant P20089-N10). We thank Klaus Hanke (Univ. of Innsbruck) for his valuable advise about the photogrammetrical survey, and all assistants during the field work on this high altitude site, especially Rainer Prinz, Lindsey Nicholson (both Univ. of Innsbruck), and Martin Kaser. Ben Marzeion, Alexander Jarosch, and Kay Helfricht (all Univ. of Innsbruck) are acknowledged for their helpful comments on structure and content of the manuscript. D. R Hardy is supported by the U.S. National Science Foundation and NOAA (CCDD and GCOS programs). We very much appreciate the local support of the Tanzanian Meteorological Agency (TMA; with special thanks to Tharsis Hyera), the Commission of Science and Technology (COSTECH), the Tanzania and the Kilimanjaro National Park Authorities (TANAPA and KINAPA), and the Tanzania Wildlife Research Institute (TAWIRI), as well as the excellent assistance of the Marangu Hotel, Moshi, TZ.

References

Bull, C. and Carnein, C. R. (1969): The mass balance of a cold glacier: Meserve Glacier, south Victoria Land, Antarctica. In: Gow, A. J. (ed.): International Symposium on Antarctic Glaciological Exploration (ISAGE). Cambridge, 77–91.

Chinn, T. J. H. (1987): Accelerated ablation at a glacier ice-cliff margin, Dry Valleys, Antarctica. In: Arctic and Alpine Research 19 (1), 71–80. DOI: 10.2307/1551002

Cullen, N. J.; Mölg, T.; Kaser, G.; Hussein, K.; Steffen, K. and Hardy, D. R. (2006): Kilimanjaro Glaciers: Recent areal extent from satellite data and new interpretation of observed 20th century retreat rates. In: Geophysical Research Letters 33, L16502. DOI: 10.1029/2006GL027084.

Diolaiuti, G.; Smiraglia, C.; Vassena, G. and Motta, M. (2004): Dry calving processes at the ice cliff of Strandline Glacier, Northern Victoria Land, Antarctica. In: Annals of Glaciology 39, 201–208.

Fitzsimons, S. J. and Colhoun, E. A. (1995): Form, structure and stability of the margin of the Antarctic ice sheet, Vestfold Hills and Bunger Hills, East Antarctica. In: Antarctic Science 7 (2), 171–179. DOI: 10.1017/S095410209500023X

Geilinger W. (1936): The retreat of the Kilimanjaro glaciers. In: Tanganyka Notes and Records 2, 7–20.

Goldthwait, R. P. (1956): Study of ice cliff in Nunatarssuaq, Greenland. In: Ohio State University Research Foundation, Technical report 11.

– (1971): Restudy of Red Rock ice cliff in Nunatarssuaq, Greenland. In: U.S. Army Cold Regions Research and Engineering Laboratory, Technical Report 224.

Greely, A. W. (1886): Three years of Arctic service: an account of the Lady Franklin Bay expedition of 1881–84, Vol. 1. London.

Hastenrath, S. (1984): The glaciers of equatorial East Africa. Dordrecht.

– (2010): Climatic forcing of glacier thinning on the mountains of equatorial East Africa. In: International Journal of Climatology 30, 146–152.

Hastenrath, S. and Greischar, L. (1997): Glacier recession on Kilimanjaro, East Africa, 1912–89. In: Journal of Glaciology 43, 455–459.

Hooke, R. L. (1970): Morphology of the ice-sheet margin near Thule, Greenland. In: Journal of Glaciology 9, 303–324.

Humphries, D. W. (1959): Preliminary notes on the glaciology of Kilimanjaro. In: Journal of Glaciology 3, 475–478.

Iqbal, M. (1983): An introduction to solar radiation. Orlando.

Jäger, F. (1931): Veränderungen der Kilimanjaro-Gletscher. In: Zeitschrift für Gletscherkunde XIX, 285–299.

Kaser, G.; Hardy, D. R.; Mölg, T.; Bradley, R. S. and Hyera, M. (2004): Modern glacier retreat on Kilimanjaro as evidence of climate change: observations and facts. In: International Journal of Climatology 24, 329–339. DOI: 10.1002/joc.1008

Kaser, G.; Mölg, T.; Cullen, N. J.; Hardy, D. R. and Winkler, M. (2010): Is the decline of ice on Kilimanjaro unprecedented in the Holocene? In: The Holocene, accepted.

Klute, F. (1920): Ergebnisse der Forschungen am Kilimandscharo 1912. Berlin.

Kraus, H. (1972): Energy exchange at air-ice interface. In: Role of Snow and Ice in Hydrology. IAHS Publication 107. Wallingford, 128–164.

Lewis, K. J.; Fountain, A. G. and Dana, G. L. (1998): Surface energy balance and meltwater production for a Dry Valley glacier, Taylor Valley, Antarctica. In: Annals of Glaciology 27, 603–609.

– (1999): How important is terminus cliff melt? A study of the Canada Glacier terminus, Taylor Valley, Antarctica. In: Global and Planetary Change 22, 105–115. DOI: 10.1016/S0921-8181(99)00029-6

Lliboutry, L. (1956): Nieves y glaciares de Chile: fundamentos de glaciologá. Santiago de Chile.

Meyer, H. (1891): Zur Kenntnis von Eis und Schnee des Kilimandscharo. In: Petermanns Geographische Mitteilungen 36, 289–294.

Mölg, T. and Hardy, D. R. (2004): Ablation and associated energy balance of a horizontal glacier surface on Kilimanjaro. In: Journal of Geophysical Research 109, D16104. DOI: 10.1029/2003JD004338

Mölg, T.; Hardy, D. R. and Kaser, G. (2003): Solar-radiation-maintained glacier recession on Kilimanjaro drawn from combined ice-radiation geometry modeling. In: Journal of Geophysical Research 108, 4731. DOI: 10.1029/2003JD003546

Mölg, T.; Cullen, N. J.; Hardy, D. R.; Kaser, G. and Klok, L. (2008): Mass balance of a slope glacier on Kilimanjaro and its sensitivity to climate. In: International Journal of Climatology 28, 881–892. DOI: 10.1002/joc.1589

Mölg, T.; Cullen, N. J.; Hardy, D. R.; Winkler, M. and Kaser, G. (2009a): Quantifying climate change in the tropical midtroposphere over East Africa from glacier shrinkage on Kilimanjaro. In: Journal of Climate 22, 4162–4181. DOI: 10.1175/2009JCLI2954.1

Mölg, T.; Chiang, J. C. H.; Gohm, A. and Cullen, N. J. (2009b): Temporal precipitation variability versus altitude on a tropical high mountain: observations and mesoscale atmospheric modelling. In: Quarterly Journal of the Royal Meteorological Society 135, 1439–1455. DOI: 10.1002/qj.461

Mölg, T.; Cullen, N. J. and Kaser, G. (2009c): Solar radiation, cloudiness and longwave radiation over low-latitude glaciers: implications for mass-balance modelling. In: Journal of Glaciology 55 (190), 292–302. DOI: 10.3189/002214309788608822

Osmaston, H. (1989): Glaciers, glaciations and equilibrium line altitudes on Kilimanjaro. In: Mahaney W. C. (ed.): Quaternary and environmental research on East African mountains. Rotterdam, 7–30.

Pettit, E. C.; Nylen, T. H.; Fountain, A. G. and Hallet, B. (2006): Ice cliffs and the terminus dynamics of polar glaciers. In: AGU Fall Meeting Abstracts C41A-0312.

Souchez, R. A. (1971): Ice-cored moraines in south-western Ellesmere Island, N. W. T., Canada. In: Journal of Glaciology 10 (59), 245–254.

Spink, P. C. (1944): Weather and vulcanic activity on Kilimanjaro. In: The Geographical Journal 103 (5), 226–229. DOI: 10.2307/1789107

Sproul, A. B. (2007): Derivation of the solar geometric relationships using vector analysis. In: Renewable Energy 32, 1187–1205. DOI: 10.1016/j.renene.2006.05.001

Thompson, L. G.; Brecher, H. H.; Mosley-Thompson, E.; Hardy, D. R. and Mark, B. G. (2009): Glacier loss on Kilimanjaro continues unabated. In: Proceedings of the National Academy of Sciences 106 (47), 19770–19775. DOI: 10.1073/pnas.0906029106

Uhlig, C. (1908): Ostafrikanische Expedition der Otto Winter-Stiftung. In: Zeitschrift der Gesellschaft für Erdkunde zu Berlin, 75–94.

White, S. E. (1958): Preliminary studies of motion of an ice cliff, Nunatarssuaq, Northwest Greenland 1955. In: Symposium de Chamonix, Publication A. I. H.

Young, A. T. (1994): Air mass and refraction. In: Applied Optics 33 (6), 1108–1110. DOI: 10.1364/AO.33.001108

Authors

Mag. Michael Winkler
Prof. Dr. Georg Kaser
Dr. Thomas Mölg

Tropical Glaciology Group
Center of Climate & Cryosphere
Department of Geography
University of Innsbruck
Innrain 52
6020 Innsbruck
Austria
michael.winkler@uibk.ac.at
georg.kaser@uibk.ac.at
thomas.moelg@uibk.ac.at

Dr. Nicolas J. Cullen
Department of Geography
University of Otago
Dunedin
New Zealand
njc@geography.otago.ac.nz

Prof. Douglas R. Hardy
Climate System Research Center
Department of Geosciences
University of Massachusetts-Amherst
Amherst, MA
USA
dhardy@geo.umass.edu

Prof. W. Tad Pfeffer
University of Colorado at Boulder
INSTAAR
Boulder, CO
USA
Tad.Pfeffer@colorado.edu